Articles

Thermal and Conformational Stability of Seed Coat Soybean Peroxidase

J. K. Amisha Kamal and Digambar V. Behere*

Department of Chemical Sciences, Tata Institute of Fundamental Research, Homi Bhabha Road, Colaba, Mumbai 400 005, India

Received February 1, 2002; Revised Manuscript Received April 30, 2002

ABSTRACT: Soybean peroxidase (SBP) obtained from the soybean seed coats belongs to class III of the plant peroxidase superfamily. Detailed circular dichroism and steady state fluorescence studies have been carried out to monitor thermal as well as denaturant-induced unfolding of SBP and apo-SBP. Melting of secondary and tertiary structures of SBP occurs with characteristic transition midpoints, T_m, of 86 and 83.5 °C, respectively, at neutral pH. Removal of heme resulted in greatly decreased thermal stability of the protein (T_m = 38 °C). The $\Delta G°(H_2O)$ determined from guanidine hydrochloride-induced denaturation at 25 °C and at neutral pH is 43.3 kJ mol^{-1} for SBP and 9.0 kJ mol^{-1} for apo-SBP. Comparison with the reported unfolding data of the homologous enzyme, horseradish peroxidase (HRP-C), showed that SBP exhibits significantly high thermal and conformational stability. We show that this enhanced structural stability of SBP relative to HRP-C arises due to the unique nature of their heme binding. A stronger heme−apoprotein affinity probably due to the interaction between Met37 and the C8 heme vinyl substituent contributes to the unusually high structural stability of SBP.

Peroxidases (oxidoreductase, EC 1.11.1.7) catalyze oxidation of a large variety of substrates by hydrogen peroxide (*1*, *2*). They have been implicated in a variety of physiological processes in plants, such as lignin biosynthesis, extensin polymerization, auxin metabolism, disease resistance, wound healing, and the response to air pollutant stress (*3*). Seed coat soybean peroxidase (SBP)[1] belongs to class III of the plant peroxidase superfamily that also includes horseradish (HRP), barley (BP1), and peanut (PNP) peroxidases (*4*). SBP is a 326-amino acid containing glycoprotein with a molecular mass of ∼37 kDa (*3*, *5*, *6*). The three-dimensional crystal structure of SBP has recently been published (Figure 1) (*7*). Superposition and structural alignment of the crystal structures of the class III plant peroxidase have shown (*7*) that SBP and HRP-C possess strikingly similar overall protein structure with a degree of sequence homology of 57%. Their common features include Fe(III) protoporphyrin IX (heme) as the prosthetic group, catalytic mechanism, conserved catalytic residues, four disulfide bonds, two Ca^{2+} binding sites located distal and proximal to heme, eight glycans, and a single tryptophan (Trp117) (*4*, *7*−*9*). The heme cavity of

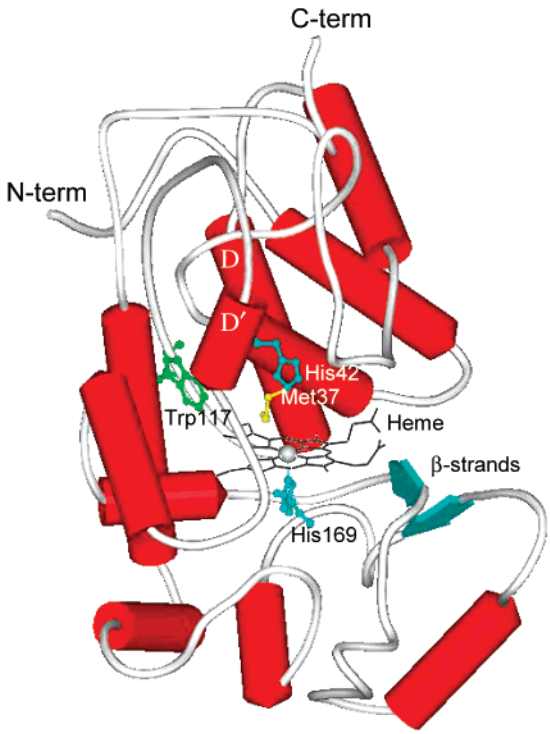

FIGURE 1: Schematic structure of SBP obtained from the crystallographic results (PDB entry 1fhf). The sketch was made using *WebLab ViewerPro*, version 3.7 (MSI).

* To whom correspondence should be addressed: Department of Chemical Sciences, Tata Institute of Fundamental Research, Homi Bhabha Road, Colaba, Mumbai 400 005, India. Phone: (91 22) 215 2971. Fax: (91 22) 215 2110. E-mail: behere@tifr.res.in.

[1] Abbreviations: SBP, seed coat soybean peroxidase; HRP-C, horseradish peroxidase isoenzyme C; heme, Fe(III) protoporphyrin IX; GdnHCl, guanidine hydrochloride; DTT, dithiothreitol; SDS−PAGE, sodium dodecyl sulfate−polyacrylamide gel electrophoresis; UV, ultraviolet; ϵ, extinction coefficient (a subscript indicates the value at that wavelength); CD, circular dichroism; $[\theta]$, molecular ellipticity (a subscript indicates the value at that wavelength); λ_{ex}, excitation wavelength; λ_{em}, emission wavelength; T, temperature; T_m, midpoint of the thermal unfolding curve; $\Delta G°$, Gibbs free energy of protein unfolding; m_G, dependence of the Gibbs free energy of unfolding on denaturant concentration; C_m, midpoint of the denaturant unfolding curve.

10.1021/bi025621e CCC: $22.00
Published on Web 06/25/2002

SBP has a hydrogen bonding network between the distal water molecules and the key residues, which, through the propionyl groups of the heme, is extended toward the proximal side of the cavity (*7*), a feature common to HRP-C and many other class III plant peroxidases.

The most widely studied member of this peroxidase family is HRP, which has found many diagnostic, biosensing, and biotechnological applications because of its high stability in aqueous solution (*10*, *11*). Unlike other class III plant peroxidases, however, SBP has been reported to show unusually high thermal stability (*12*). Hence, it particularly shows promise as a biocatalyst and biosensor (*13*−*15*) and shows potential applications in nonphysiological processes such as wastewater treatment and phenolic resin synthesis (*12*, *16*). SBP has been reported to be less susceptible to both heme loss (*12*) and permanent inactivation by hydrogen peroxide (*16*) than HRP-C. It does not undergo any heat inactivation below 70 °C even after up to 12 h (*12*). The enzyme is active under acidic conditions as well as in a variety of organic solvents (*12*). It is present in large amounts in the soybean seed coats, which is an inexpensive source that is readily available (*3*). These attributes of the enzyme make it an attractive candidate for industrial use. It is found that SBP is superior to HRP to help diagnose various viral, bacterial, and parasitic diseases, including AIDS and malaria. Medical diagnosing kits with SBP being the integral part are in the market now. However, very little spectroscopic structural information has been reported for this enzyme. Recently, electronic absorption and resonance Raman spectral studies (*4*, *17*) focusing on the heme coordination state of SBP have been reported. Most recently, we have reported tryptophan fluorescence studies on SBP and apo-SBP (*18*). Apart from the preliminary investigations on thermal stability of SBP (*12*), no further detailed studies with regard to the unfolding of the enzyme have been reported. The conformational stability of SBP, i.e., how much more stable the folded, globular conformation is than unfolded conformations, is not known so far. The presence of four disulfide bonds and a heme prosthetic group makes SBP an excellent model for studying energetics and mechanism of protein folding. Physicochemical studies of the heme group can provide insight into the structure−activity relationship of the enzyme. The objectives of this study were to study its spectroscopic and physicochemical properties under various conditions of pH, temperature, and treatment of urea and guanidine hydrochloride (GdnHCl) using UV−visible, circular dichroism, and steady state fluorescence techniques to understand the thermal and conformational stability of the enzyme. The results are explained with possible comparisons with HRP-C to probe the nature of the additional stabilizing elements in SBP.

MATERIALS AND METHODS

SBP (salt free lyophilized powder), HRP-C ($R_Z > 3.1$, salt free lyophilized powder), DEAE Sepharose CL-6B, urea, GdnHCl, and DTT were purchased from Sigma Co. Deionized water (PURITE RO 50) was used in all the experiments. A series of McIlvaine citrate−phosphate buffers (*19*) with pHs ranging from 3 to 9.2 having a constant ionic strength ($I = 0.25$ M) were used in all the experiments. All other chemicals that were used were of the highest purity.

Purification of SBP and Preparation of Apo-SBP. Crude SBP ($R_Z = A_{403}/A_{280} \approx 0.5$) (∼50 mg) was dissolved in a minimum volume of 25 mM KH_2PO_4 buffer (pH 7.0) and applied onto a 2.5 cm × 12 cm column of DEAE Sepharose CL-6B equilibrated with the same buffer. The protein bound to the column was washed thoroughly with the equilibrating buffer and eluted using linear gradient of 0 to 0.5 M KCl (800 mL). Pooled fractions with an R_Z value higher than 2.3, after concentration, were dialyzed overnight against two changes of the buffer and applied onto the regenerated DEAE Sepharose CL-6B column, and subsequently, processes were repeated as described above. The enzyme that was obtained had an R_Z value of 2.8−3.0 at the end of the second cycle of the purification process that ensured 6-fold purity. SDS−PAGE (10% polyacrylamide) showed a single band corresponding to SBP. The heme content of the purified protein was determined using a $\Delta\epsilon$ ($\epsilon_{557} - \epsilon_{541}$) of 20.7 mM^{-1} cm^{-1} from the dithionite-reduced minus ferricyanide-oxidized pyridine hemochrome spectra (*20*). The extinction coefficient determined at 403 nm ($\epsilon_{403} = 94.6$ mM^{-1} cm^{-1}) is close to the earlier reported value ($\epsilon_{403} = 90.0$ mM^{-1} cm^{-1}) for SBP (*9*), and was used to determine the concentration of purified enzyme samples. The value also compares well with the ϵ_{403} value (102 mM^{-1} cm^{-1}) of HRP-C (*2*). The prosthetic heme group of SBP was removed by Teale's acid butanone procedure (*21*) to yield apo-SBP. ϵ_{280} was determined to be 24 mM^{-1} cm^{-1} from the extinction coefficient values of tryptophan, tyrosine, and cysteine (*22*) and was used to determine the concentration of apo-SBP.

Unfolding Studies. Unfolding of the enzyme was monitored by both circular dichroism and tryptophan fluorescence techniques. CD experiments were carried out using a Jasco J600 spectropolarimeter. CD in the 200−250 nm region (far-UV CD) was monitored using a rectangular cuvette with a path length of 1 mm placed on a thermostated cell holder attached to a thermometer with a protein concentration of 6 μM. CD in the 250−350 nm region (near-UV CD) and in the 350−500 nm region (Soret CD) were monitored using a water-jacketed cylindrical cuvette with a path length of 10 mm with a protein concentration of 15 μM. The CD data were expressed in terms of molecular ellipticity, [θ], in degrees square centimeter per decimole. Fluorescence measurements were carried out using Spex Fluorolog-dM3000F spectrofluorimeter using a cuvette with a path length of 10 mm. To minimize contributions of the tyrosine residues present in the sample, a λ_{ex} of 295 nm was used (*23*). Emission spectra were recorded in the wavelength range of 300−450 nm.

For thermal unfolding studies, the temperature was increased from 20 to 88 or 95 °C with a heating rate of 0.5 °C/min. Modification of SBP by DTT was achieved by incubating the protein solution containing excess (13 mM) DTT for 23 h at 4 °C following the reported procedure (*24*). Thermal unfolding at fixed GdnHCl concentrations (0, 5.8, 6.3, 6.9, and 8 M) at pH 7.0 was monitored by recording far-UV CD spectra in the temperature range of 25−95 °C. At the end of each thermal unfolding experiment, the sample was cooled immediately to room temperature and spectra were recorded to know the extent of refolding. Temperature-dependent fluorescent changes were calibrated against a control of the completely denatured enzyme.

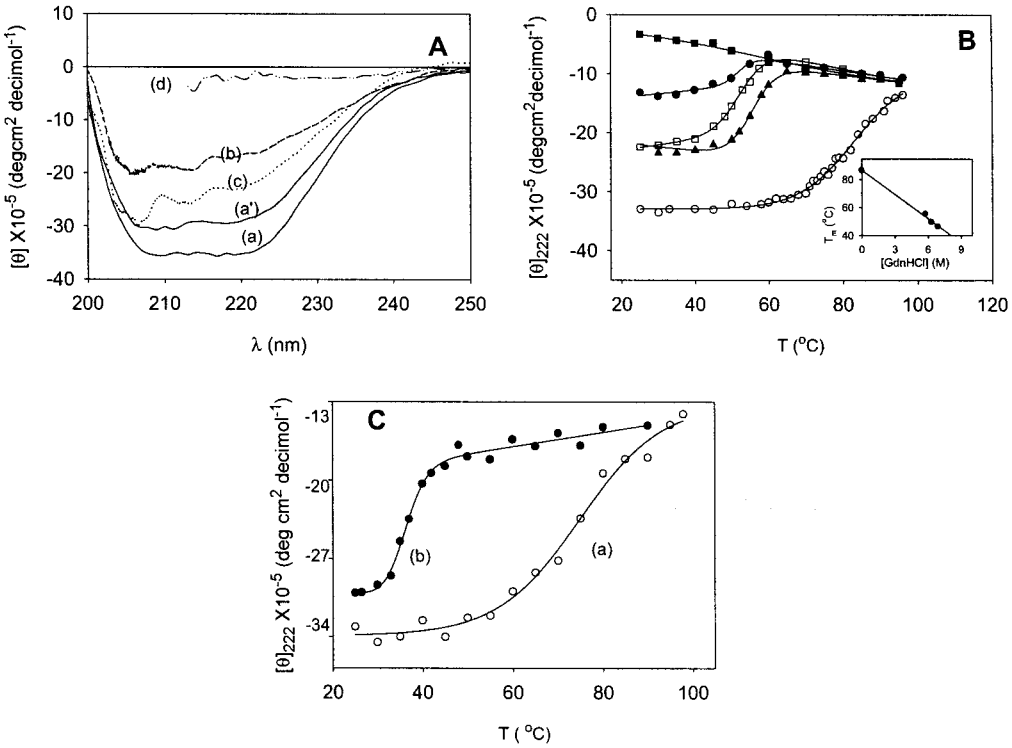

FIGURE 2: (A) Far-UV CD spectra of SBP at 25 °C (a), apo-SBP at 25 °C (a′), SBP at 92 °C (b), SBP after cooling to 25 °C from 92 °C (c), and SBP in the presence of 8 M GdnHCl at 25 °C (d). (B) Temperature dependencies of $[\theta]_{222}$ of SBP at pH 7.0 in the absence of denaturant (○), in 5.8 M GdnHCl (▲), in 6.3 M GdnHCl (□), in 6.9 M GdnHCl (●), and in 8.0 M GdnHCl (■). Solid lines represent sigmoidal fits to the data. The inset is the melting temperatures of SBP for various GdnHCl concentrations (0−6.9 M). (C) Temperature dependencies of $[\theta]_{222}$ at pH 7.0 of SBP treated with 13 mM DTT (○) and apo-SBP (●). Solid lines represent sigmoidal fits to the data.

For denaturant unfolding studies, a stock of 8−8.3 M GdnHCl was used. The GdnHCl concentration in the stock solution was determined using a refractometer according to the reported method (*25*). Protein solutions were equilibrated with various GdnHCl concentrations, ranging from 0 to 8 M for 23 h at room temperature before the spectra were recorded. The reversibility was checked by dissolving the protein in a high denaturant concentration, followed by equilibration for 23 h, dilution into the buffer solution, and then equilibration for an additional 23 h before the spectra were recorded.

Data Analysis. In GdnHCl-induced unfolding experiments, thermodynamic properties of SBP and apo-SBP were calculated assuming a two-state denaturation process (*25*). Unfolding curves of SBP were fitted to a nonlinear least-squares analysis by using the equation (*26*)

$$Y_0 = \frac{Y_F + m_F[D] + (Y_U + m_U[D])\exp\left\{\frac{-[\Delta G°(H_2O) + m_G[D]]}{RT}\right\}}{1 + \exp\left\{\frac{-[\Delta G°(H_2O) + m_G[D]]}{RT}\right\}} \quad (1)$$

where Y_0 is the value of the spectroscopic property of protein at a given GdnHCl concentration, [D]; Y_F and Y_U represent the intercepts and m_F and m_U the slopes of the native and unfolded baselines, respectively; m_G is a measure of the dependence of $\Delta G°$ on GdnHCl concentration; and $\Delta G°(H_2O)$ is the free energy change in the absence of denaturant. The midpoint of denaturation, C_m, corresponds to the GdnHCl concentration where $\Delta G° = 0$. GdnHCl-induced unfolding curves of apo-SBP were analyzed by linear least-squares analysis, by using the equation (*25*)

$$\Delta G° = \Delta G°(H_2O) + m_G[D] \quad (2)$$

RESULTS

Thermal Unfolding of SBP and Apo-SBP Monitored by Far-UV CD. Far-UV CD of a protein conforms to its secondary structure. Far-UV CD spectra of SBP at 25 and 92 °C are shown as traces a and b of Figure 2A, respectively. $[\theta]$ decreases when $T \geq 60$ °C and levels off when $T \geq 90$ °C, indicating thermal unfolding of SBP. Upon cooling to 25 °C, the protein refolded to a state with decreased ellipticity compared to the native state (trace c of Figure 2A). As seen in trace b of Figure 2A, SBP at 92 °C shows some residual ellipticity ($[\theta]_{222} \sim -14 \times 10^5$ deg cm^{-2} dmol^{-1}). SBP treated with an excess of DTT (13 mM) at 92 °C also exhibits the same residual ellipticity, indicating that this high-temperature state is not arising due to stabilization of the protein structure due to disulfide bonds. In 8 M GdnHCl at 25 °C, the CD intensity is nearly zero (trace d of Figure 2A), an indication of the total unfolding of secondary structure.

To understand the nature of the "high-temperature state" and the effect of GdnHCl on the thermal denaturation of SBP, temperature dependences of $[\theta]_{222}$ of SBP in the presence of fixed GdnHCl concentrations at pH 7.0 in the range of 0−8 M were studied (Figure 2B). Melting of the secondary structure of SBP occurs with an apparent T_m value of 86 °C in the absence of any denaturant (Figure 2B). There is good coincidence between the thermally induced unfolded states in the absence and presence of GdnHCl. Molecular

ellipticity values converge to an approximately same final $[\theta]_{222}$ value of -14×10^5 deg cm^{-2} dmol^{-1}. As the GdnHCl concentration increases, the unfolding transition occurs at lower temperatures. The values of T_m were found to be 55, 50, and 46 °C at 5.8, 6.3, and 6.9 M GdnHCl, respectively. The inset of Figure 2B shows that the T_m varies linearly with the GdnHCl concentration. These observations suggest that the enzyme attains a completely unfolded state by both thermal and GdnHCl denaturation pathways and that the unfolded state is characterized by a zero CD signal at room temperature but acquires residual CD intensity at elevated temperatures, the magnitude of which is independent of GdnHCl concentration. Residual ellipticity at elevated temperatures, characteristic of a completely unfolded state, has been previously observed for barstar (*26*) and *Escherichia coli* dihydrofolate reductase (*27*).

The CD spectra of DTT-treated SBP and apo-SBP at 92 °C and after cooling to 25 °C superimposed with the corresponding spectra of SBP. While refolded SBP retains ~65% of the ellipticity before heating (like DTT-treated SBP), apo-SBP retains ~80% (see Figure 2A). These observations indicate that (i) SBP, DTT-treated SBP, and apo-SBP attain the same unfolded state when $T \geq 90$ °C, (ii) unfolding of SBP and apo-SBP is largely reversible (however, a small part of the total protein molecules underwent irreversible thermal aggregation), and (iii) heme may be lost irreversibly from the native enzyme at elevated temperatures, thus exhibiting a refolded state identical to that of apo-SBP. The partial irreversibility of thermal backbone unfolding of SBP and apo-SBP suggests an N $\rightleftharpoons$ U $\rightarrow$ F mechanism in general, known as the Lumry and Eyring model (*28*). According to this model, the reversible denaturation step from the native (N) to the unfolded state (U) is followed by a slow monomolecular aggregation of the denatured protein (F).

It is seen from Figure 2B that the cooperativity of the unfolding transition of SBP in the absence of GdnHCl is very low when compared to those in the presence of 5.8, 6.3, and 6.9 M GdnHCl (*29*), indicating that the N $\rightleftharpoons$ U transition in the absence of GdnHCl proceeds through a number of partly folded structures (*29*, *30*). None of these intermediates accumulate in sufficient amounts to form a separate transition.

Thermal stabilities of SBP and HRP-C can be compared by comparing their T_m values (*31*). The fact that the T_m for SBP (86 °C) is relatively higher than that reported for HRP-C (74 °C) (*11*) signifies relatively enhanced thermal backbone stability of SBP. The temperature dependence of $[\theta]_{222}$ of DTT-modified SBP at neutral pH (trace a of Figure 2C) showed a lower transition temperature ($T_m = 75$ °C), indicating that reduction of interhelical disulfide bonds significantly decreases the thermal stability of the enzyme. For HRP-C, T_m decreases to 65 °C on treatment with DTT (*11*). Thus, the extent of the decrease in thermal stability is almost the same for both SBP (~13%) and HRP-C (~12%), indicating that the contributions of the four interhelical disulfide bridges to the stability of the two proteins are comparable. Curve b of Figure 2C is the temperature dependence of $[\theta]_{222}$ of apo-SBP, showing a T_m of 38 °C. The drastic decrease in T_m upon removal of heme indicates the dominant role of heme in enhancing the protein backbone stability. Thus, the contribution to the thermal stability of

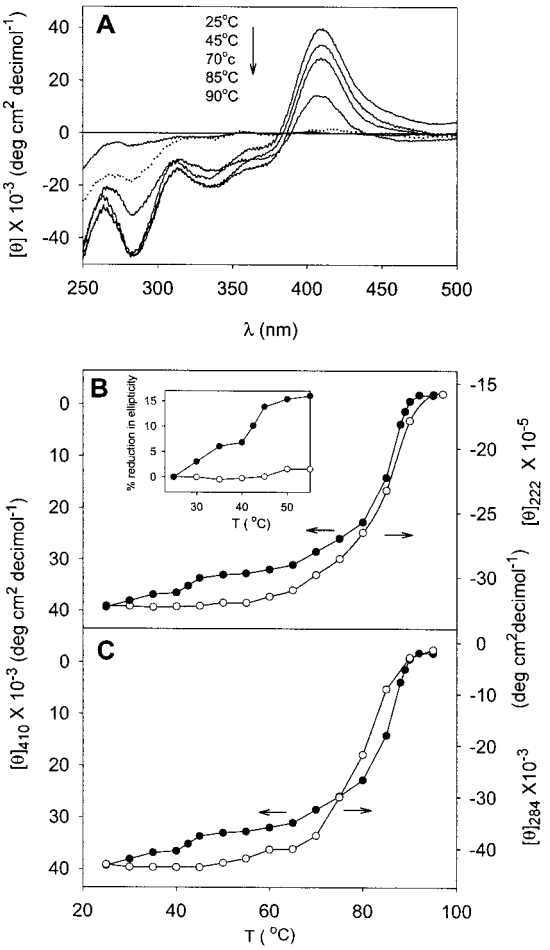

FIGURE 3: (A) CD spectra in the 250−500 nm region of SBP at different temperatures. The dotted line represents the spectrum of SBP cooled to 25 °C from 92 °C. (B) Temperature dependencies of $[\theta]_{410}$ (●) and $[\theta]_{222}$ (○) at pH 7.0. The inset is the first part of the curves in more detail. (C) Temperature dependencies of $[\theta]_{410}$ (●) and $[\theta]_{284}$ (○) at pH 7.0.

SBP due to the heme group amounts to ~56%. The cooperativity of the unfolding transition in apo-SBP is very high when compared to that in SBP, indicating that the N $\rightleftharpoons$ U transition in apo-SBP is a simple two-state process. The thermal unfolding characteristics of apo-SBP are very similar to those of apo-HRP-C ($T_m = 40$ °C) (data not shown).

Thermal Unfolding of SBP Monitored by Near-UV CD and Soret CD. CD in the near-UV region and CD in the Soret region were monitored to determine the effect of temperature on the overall protein tertiary structure and tertiary structure around the heme active site, respectively. Temperature-dependent CD spectra of SBP in 250−500 nm spectral range are shown in Figure 3A. The positive intensity of the Soret CD band centered around 410 nm decreases as the temperature increases and vanishes when $T \geq 90$ °C, an indication of the complete removal of heme from the heme cavity at these elevated temperatures. The absence of a Soret CD band for the sample cooled to room temperature indicates that the heme loss is irreversible. The temperature dependence of $[\theta]_{410}$ is shown in panels B and C of Figure 3. The curves show a reproducible kink at 40−47 °C. This transition phase is reversible and is associated with a T_m of 43 °C at pH 7.0. A similar transition was observed for HRP-C having a T_m of 45 °C (*11*). However, the total reduction in the

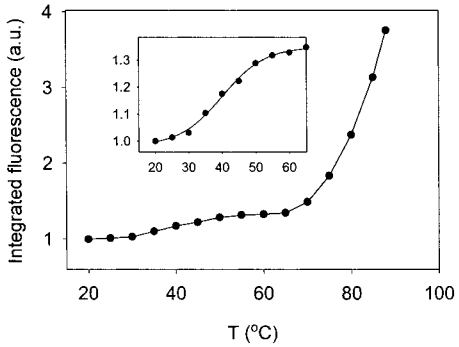

FIGURE 4: Temperature dependence of the relative integrated tryptophan fluorescence intensity (306−400 nm) of SBP. The inset is the first part of the curve in more detail.

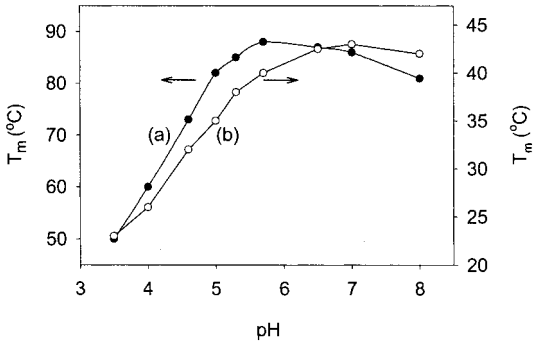

FIGURE 5: pH dependence of T_m corresponding to the melting of the secondary structure monitored by $[\theta]_{222}$ (●) and of the tertiary structure around heme monitored by fluorescence (○) for SBP.

ellipticity observed during this transition in SBP is relatively very small (∼13%, inset of Figure 3B) compared to that reported in HRP-C (∼30%) (*11*). This indicates that the heme cavity is relatively more ordered or structured in SBP than in HRP-C. At higher temperatures, the process of heme falling out of the protein occurs with a characteristic T_m of 85 °C (Figure 3B,C). This significantly higher T_m for the heme depletion in SBP compared to that of HRP-C (74 °C) (*11*) indicates that the heme pocket in SBP is more resistant to thermal denaturation than in HRP-C. This enhanced stability of the heme cavity of SBP is consistent with the observation of increased orderedness.

The overall tertiary structure of SBP is lost when $T \geq 90$ °C as the magnitude of the negative intensity of the CD band centered on 284 nm attains the minimum value (Figure 3A). The thermal unfolding curve of $[\theta]_{284}$ shows a characteristic T_m of 83.5 °C (Figure 3C). This T_m value is very close to that of backbone melting (Figure 3B) and the heme detachment process (Figure 3C), indicating that these three processes are occurring almost simultaneously in SBP.

Thus, unlike the melting of the backbone or overall tertiary structure of the protein, thermal unfolding of the tertiary structure around the heme cavity passes through an initial reversible phase and thus clearly shows the existence of one stable intermediate state, denoted as I. The Soret ellipticity value of this intermediate is very close to that of the native enzyme (∼87%, Figure 3B), indicating that it is structurally closer to the native state (N) than to the unfolded state (U). This intermediate is characterized by intact secondary (Figure 3B) and overall tertiary (Figure 3C) structures. To understand more about this intermediate state as well as to monitor the unfolding of SBP with a different perspective, the temperature dependence of the intrinsic tryptophan fluorescence of SBP was determined.

Thermal Unfolding of SBP Monitored by Tryptophan Fluorescence. The fluorescence of tryptophan in SBP is highly quenched due to Förster resonance energy transfer to the bound heme (*18*). Any conformational change in the heme cavity, if accompanied by a change in the heme orientation and/or a change in its relative distance from tryptophan, affects the quenching efficiency and may result in observable variations in tryptophan fluorescence intensity (*10*, *11*). The temperature dependence of the integrated area under the fluorescence emission spectrum is shown in Figure 4. The unfolding has an initial reversible phase associated with the formation of a stable intermediate with a T_m of 43 °C. The increase in the fluorescence intensity when the temperature is increased from 20 to 60 °C is only 1.3-fold (Figure 4), which is very low (∼10%) compared to the 4-fold enhancement when the temperature reaches 88 °C. These observations taken together with that of the temperature dependence of Soret CD (see Figure 3) indicate that the intermediate observed in both cases is identical and is characterized by an altered heme cavity structure. At 55−65 °C, SBP was reported (*32*) to show the same activity as that shown at 23−25 °C. These features of the intermediate state indicate that it is structurally and functionally very close to the native enzyme. The sharp increase in fluorescence intensity observed above 65 °C (Figure 4) results from the considerable reduction in the level of heme quenching accompanying unfolding (*23*, *25*) of the secondary and tertiary structures of SBP.

pH Dependence of the Thermal Unfolding of SBP. The pH dependence of T_m of the melting of the backbone and the intermediate of SBP is shown in Figure 5. A pronounced decrease in the T_m values observed below pH 5 indicates a considerable decrease in the protein stability due to the weakening of hydrogen bonds. It is noted from curve a that the thermal backbone stability of SBP is optimal at pH ∼5.5 (88 °C), the pH at which catalytic activity is also reported to be optimal (*33*). The transition curve of trace b of Figure 5 gives a pK_a of ∼4.5. This pK_a corresponds to protonation of distal histidine(s) (His40/42). The T_m value close to room temperature at pH <4 indicates that residues like histidine become protonated, thus breaking the hydrogen bonding network of the heme cavity. This suggests that the stable intermediate state observed in thermally induced heme cavity unfolding is associated with breaking of the hydrogen bonding network involving the distal histidine in the heme pocket. The pH dependence of the melting of the intermediate is similar to that observed in HRP-C (*11*), indicating that the extents of hydrogen bond stabilization of the heme cavity of these two proteins are comparable. The observation of significant ellipticity in the Soret region for this intermediate (see Figure 3) indicates that though the hydrogen bonds are disrupted, heme remains attached to the protein with a considerable retention of order in the heme cavity. This may be attributed to the unbroken Fe−His169 bond (Figure 1) at these temperatures (up to ∼70 °C) which is normally broken at pH <3.0 at room temperature as well as to the hydrophobic interactions that hold the heme in the hydrophobic core of the protein which normally do not vanish with an increase in temperature.

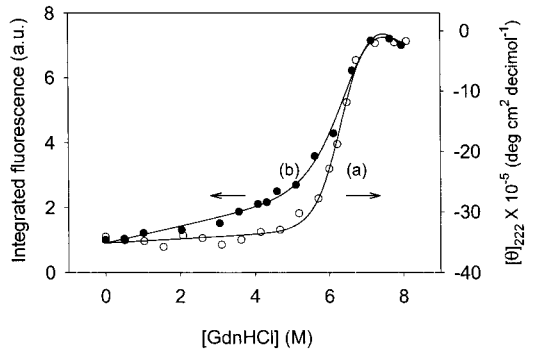

FIGURE 6: Guanidine hydrochloride-induced unfolding curves of SBP monitored by $[\theta]_{222}$ (○) and integrated tryptophan fluorescence intensity (306−400 nm) (●). Solid lines represent fits to the data according to eq 1.

Table 1: Thermodynamic Parameters Governing GdnHCl Unfolding at pH 7.0 and at 25 °C

protein	probe	$\Delta G°(H_2O)$ (kJ mol^{-1})	m_G (kJ mol^{-1} M^{-1})	C_m (M)
SBP	$[\theta]_{222}$	43.3 ± 2.4	6.67 ± 0.36	6.5
	Trp fluorescence	34.9 ± 2.4	5.11 ± 0.81	6.0
apo-SBP	$[\theta]_{222}$	7.8	3.3	2.0
	Trp fluorescence	9.0	34.6	0.24
HRP-C[a]	$[\theta]_{222}$	16.7 ± 2.5	8.37	2.0
	Trp fluorescence	biphasic	−	−
apo-HRP-C[a]	$[\theta]_{222}$	7.6	4.6	1.8
	Trp fluorescence	9.2	34.3	0.3

[a] Data for HRP-C and apo-HRP-C are from Tsaprailis et al. (*19*) and Pappa and Cass (*30*), respectively.

GdnHCl-Induced Unfolding of SBP Monitored by Far-UV CD. The conformational stability of a protein can be probed by monitoring equilibrium unfolding using denaturants such as urea or GdnHCl (*25*). SBP, upon incubation in 9.8 M urea for 23 h, underwent only 11−12% reduction in backbone CD signal (data not shown); however, the complete loss of secondary structure was observed when incubated in ≥7.5 M GdnHCl (see Figure 2A) for 23 h. The degree of reversibility was found to be ∼90%. Curve a of Figure 6 is the plot of $[\theta]_{222}$ of SBP versus GdnHCl concentration for the data collected at pH 7.0 and 25 °C. The sigmoidal change observed in a quite narrow GdnHCl concentration range of 5−7.5 M suggests a cooperative two-state transition. The calculated fit to the data according to eq 1 yielded a $\Delta G°(H_2O)$ value of 43.3 ± 2.4 kJ mol^{-1}. This value lies in the middle of the range of values (21−63 kJ mol^{-1}) described for globular proteins (*34*), suggesting substantial conformational stability of SBP. The value, however, is much higher compared to that reported for HRP-C (∼17 kJ mol^{-1}, Table 1), indicating that the conformational stability of SBP is 2.5-fold greater than that of HRP-C. The midpoint of the unfolding transition, C_m, is 6.5 M, a value very high compared with the value of HRP-C (2.0 M, Table 1), indicating the increased resistance of SBP for unfolding. The obtained m_G value is 6.67 ± 0.36 kJ mol^{-1} M^{-1} for SBP. m_G is a measure of the surface area exposed to solvent upon unfolding and is proportional to the number and type of groups that are freshly exposed to solvent when the protein unfolds (*27*, *35*). SBP and HRP-C, however, have m_G values with comparable magnitudes (Table 1) which points to the compositional and structural similarities in them. This is consistent with the X-ray crystal structures of these two proteins (*7*, *8*). Further, the large difference in $\Delta G°(H_2O)$ values between these two enzymes solely reflects the difference in their C_m values. Therefore, the enhanced stability of SBP, indicated by the increased resistance to the denaturant, relates to the extra stabilizing elements in SBP, and any contribution to the extra stability of SBP relative to that of HRP-C due to the difference in their amino acid composition and/or conformation may be very small.

GdnHCl-Induced Unfolding of SBP Monitored by Tryptophan Fluorescence. To complement the CD experiments, we used the intrinsic fluorescence of Trp117 to study the unfolding of SBP as a function of GdnHCl concentration. The λ_{em} shifted gradually from 335 nm in 0 M GdnHCl to 355 nm in ≥7.5 M GdnHCl at pH 7.0 and 25 °C (data not shown). This λ_{em} is typical for a fully solvent exposed tryptophan (*18*, *23*). The increase in quantum yield observed due to the relief of heme quenching is ∼7-fold. Curve b of Figure 6 is the GdnHCl unfolding curve of SBP monitored by fluorescence. The obtained $\Delta G°(H_2O)$ value is 34.9 ± 2.4 kJ mol^{-1}, which is low compared to the value obtained from CD experiments (Table 1). The disagreement between these two values [$\Delta\Delta G°(H_2O) \sim 8$ kJ mol^{-1}] indicates that the unfolding involves at least one stable intermediate and that the free energy change between the native state and this intermediate state is ∼35 kJ mol^{-1}. It has been reported (*10*, *30*) for HRP-C that the fluorescence monitored unfolding shows a second transition after the total loss of secondary structure at ≥4 M GdnHCl. Therefore, it is suggested that this intermediate of SBP might be similar to that of HRP-C. This intermediate is associated with a complete loss of secondary structure but an altered tryptophan environment such that the second transition could be the relaxation of the tryptophan-containing loop during the detachment of heme from the peptide chain (*10*, *30*). Therefore, on the basis of CD and fluorescence experiments, GdnHCl unfolding of SBP can be best described by the mechanism

$$N \rightleftharpoons U' \rightleftharpoons U \qquad (3)$$

where the intermediate state U′ is devoid of secondary structure which needs an energy input of $\Delta\Delta G°(H_2O)$ of ∼8 kJ mol^{-1} to unfold further to state U, and therefore may have the structural characteristics closer to those of the denatured state than to those of the native state.

GdnHCl-Induced Unfolding of Apo-SBP Monitored by Far-UV CD and Tryptophan Fluorescence. The λ_{em} of apo-SBP shifted from 340 to 355 nm when the GdnHCl concentration was increased from 0 to 7.5 M (data not shown). Curves a and b of Figure 7A represent GdnHCl-induced unfolding profiles of apo-SBP monitored by $[\theta]_{222}$ and tryptophan fluorescence, respectively. It is seen from curve a that the protein has intact secondary structure up to 0.4 M GdnHCl. Curve b shows that the fluorescence quantum yield is maximum (2.5-fold) around 0.4−0.6 M GdnHCl. A transition similar to that of fluorescence is observed in the aromatic region monitored by $[\theta]_{280}$ (data not shown). These observations indicate the existence of at least one stable intermediate (I) at ∼0.4 M GdnHCl characterized by intact secondary structure, but with collapsed tertiary structure. The unfolding of apo-SBP is reversible, and the denaturation curves were analyzed by eq 2. As seen in Figure 7B and Table 1, the $\Delta G°(H_2O)$ values obtained by both $[\theta]_{222}$ and

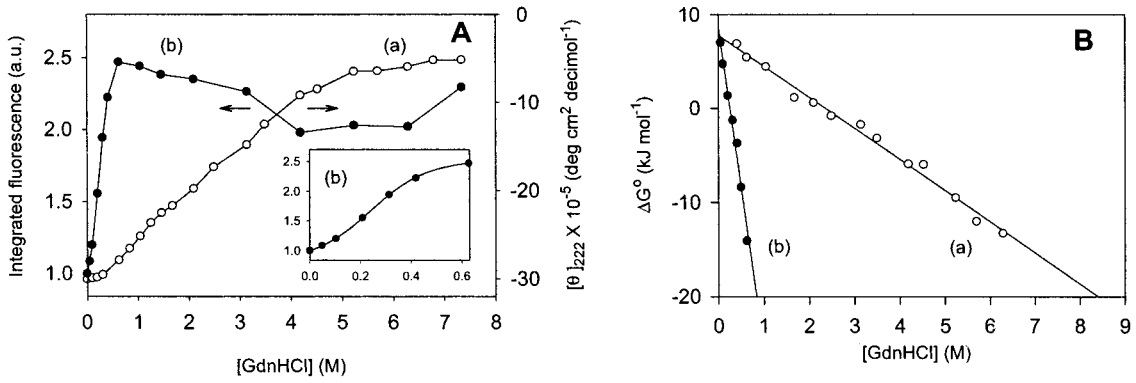

FIGURE 7: (A) Guanidine hydrochloride-induced unfolding curves of apo-SBP monitored by $[\theta]_{222}$ (○) and integrated tryptophan fluorescence intensity (306−450 nm) (●). The inset shows the first part of the fluorescence-monitored unfolding curve in more detail. (B) $\Delta G°$ for apo-SBP as a function of guanidine hydrochloride concentration as estimated from $[\theta]_{222}$ (○) and integrated tryptophan fluorescence intensity (●). Solid lines represent fits to the data according to eq 2.

tryptophan fluorescence are more or less similar. The very low $\Delta G°(H_2O)$ value of apo-SBP (9.0 kJ mol^{-1}) compared to that of SBP suggests the dominant role of heme in the conformational stability of the enzyme. Thus, the contribution to the conformational free energy of SBP due to the heme prosthetic group amounts to ~80%. The m_G value, and thus the cooperativity of unfolding, of apo-SBP obtained by $[\theta]_{222}$ is too low when compared to that calculated from tryptophan fluorescence (Table 1), consistent with the shape of the individual unfolding curves (Figure 7A). These results indicate that the unfolding of apo-SBP begins with the loss of tertiary structure occurring in a simple two-state manner, followed by the backbone unfolding proceeding through a number of distinct partly folded structures. Therefore, on the basis of CD and fluorescence experiments, the unfolding mechanism that describes, in general, the denaturant unfolding of apo-SBP is

$$N \rightleftharpoons I \rightleftharpoons U \quad (4)$$

The unfolding curves shown in Figure 7A and the deduced thermodynamic parameters are similar to those reported for apo-HRP-C (Table 1) (*30*). This indicates that the mechanisms of unfolding and conformational stabilities of these two apo proteins are the same.

DISCUSSION

The stability estimate of a protein is very often based on the analysis of denaturant-induced or thermally induced unfolding transitions, measured either spectroscopically or calorimetrically. Thermal unfolding of the backbone as monitored by $[\theta]_{222}$ and the overall tertiary structure of SBP as monitored by $[\theta]_{284}$ individually follow the $N \rightleftharpoons U \rightarrow F$ mechanism, whereas unfolding of the tertiary structure around the heme cavity as monitored by $[\theta]_{410}$ follows the $N \rightleftharpoons I \rightarrow F$ mechanism. The reversible formation of the intermediate state, I, is followed by the irreversible heme detachment process. Fluorescence experiments further confirm the presence of the intermediate state. Taken together with the results of CD and tryptophan fluorescence experiments, the following pathway is proposed, in general, for thermal unfolding of SBP

$$N \rightleftharpoons I \rightleftharpoons U \rightarrow F \quad (5)$$

Unfolding of the native state of SBP (N) begins with the loosening of the heme cavity due to breaking of the hydrogen bonding network involving a distal histidine and proceeds to the stable intermediate state, I. This is then followed by the simultaneous loss of secondary and tertiary structures through partly folded structures ($I \rightleftharpoons U$ transition) with the immediate release of heme from the unfolded polypeptide chain.

GdnHCl-induced unfolding of SBP follows the mechanism represented by eq 3 ($N \rightleftharpoons U' \rightleftharpoons U$). While $[\theta]_{222}$-monitored unfolding of SBP is an $N \rightleftharpoons U$ transition providing the $\Delta G°(H_2O)$ of ~43 kJ mol^{-1}, tryptophan fluorescence-monitored unfolding is the $N \rightleftharpoons U'$ step providing a $\Delta G°(H_2O)$ value of ~35 kJ mol^{-1}. The $U' \rightleftharpoons U$ transition is a silent process in the $[\theta]_{222}$-monitored unfolding, as neither U′ nor U possesses any secondary structure. This transition, though, was detected in the fluorescence-monitored unfolding of HRP-C (*10*, *30*) as U′ is stable from 3 to 4 M GdnHCl and is not discernible for SBP as U′ remains stable from 7.5 M onward even up to 8 M, the maximum possible GdnHCl concentration in the protein solution under physiological conditions. However, an insight to the nature of the $U' \rightleftharpoons U$ transition in SBP is indirectly possible. Unfolded SBP (U) is expected to possess the same fluorescence emission features as unfolded apo-SBP. Apo-SBP, in the presence of 7.5 M GdnHCl, has a λ_{em} of 355 nm and a fluorescence quantum yield enhanced 2.3-fold relative to that in 0 M GdnHCl (trace b of Figure 7A). We have previously observed (*18*) that SBP undergoes a 10-fold enhancement in the fluorescence quantum yield when heme is removed. Therefore, the U state of SBP is expected to possess a λ_{em} of 355 nm and a quantum yield enhanced 23-fold relative to that of state N. Since U′ is characterized by a λ_{em} of 355 nm and a quantum yield 7-fold higher than that of N (trace b of Figure 6), the $U' \rightleftharpoons U$ transition proceeds with no shift in λ_{em} but with increasing fluorescence intensity such that U attains a quantum yield enhanced 3.3-fold relative to that of U′. These spectroscopic features can be correlated with the relaxation in the tryptophan-containing loop connecting helices D and D′ (Figure 1) during the detachment of heme from the unfolded polypeptide chain as has been suggested for HRP-C. Tryptophan is fully solvent exposed in U′, accounting for no shift in λ_{em} during the transition; however, the fluorescence quantum yield increases as heme becomes detached from the unfolded peptide chain.

GdnHCl-induced unfolding of apo-SBP follows the mechanism represented by eq 4 (N ⇌ I ⇌ U). The $\Delta G°(H_2O)$ values obtained from both $[\theta]_{222}$ (7.8 kJ mol^{-1}) and tryptophan fluorescence (9.0 kJ mol^{-1}) for apo-SBP are very similar, indicating that the unfolding of apo-SBP monitored by $[\theta]_{222}$ and tryptophan fluorescence is a direct N ⇌ U transition. While states N and I are indistinguishable in $[\theta]_{222}$, states I and U are so in tryptophan fluorescence.

The free energy change associated with protein unfolding results from a combination of the hydrophobic effect, hydrogen bonding, electrostatic interactions, close packing, and backbone and side chain configurational entropy (*36*). Apart from the contribution of various inter-residue interactions, the folded structure of a heme protein is stabilized by coordination with the heme (*37*). Since high conformational stability [i.e., a large $\Delta G°(H_2O)$ value] is not necessarily related to a high thermal stability (i.e., a large T_m value) (*38*), the causes of the conformational and thermal stability of the protein are to be treated differently. Thermostability of different proteins is achieved by a combination of individual strategies such as an increased number of hydrogen bonds and salt bridges, an optimized packing of the hydrophobic core, shortened surface loops, an increased number of prolines, and an increase in the number of buried hydrophobic residues (*38*). We observed that one of the major contributors of both thermal and conformational stability of SBP is the heme prosthetic group. An increase in conformational stability could have its origin in a decrease in the conformational free energy of the native state, an increase in the free energy of the unfolded state, or a combination of both (*31*). Binding of heme is equivalent to introducing several hydrophobic groups contributing to the hydrophobic region within the protein structure, which stabilizes the native conformation of the protein (*39*). Further, these enhanced hydrophobic interactions, with better packing of the hydrophobic core of the protein, contribute to its enhanced thermal stability.

SBP and HRP-C are very similar in their amino acid sequence and overall three-dimensional structure and therefore are homologous. However, the thermal and conformational stability of SBP are observed to be substantially higher than those of HRP-C. Nevertheless, their less stable apo analogues possess nearly identical T_m and $\Delta G°(H_2O)$ values; i.e., in the absence of bound heme, the structural stabilities of both apoproteins are the same. But when heme binds, the gains in both thermal and conformational stability for SBP (∼56 and ∼80%, respectively) are much higher than those for HRP-C (∼46 and ∼45%, respectively). Therefore, the enhanced thermal and conformational stability of SBP compared to that of HRP-C is due to the unique nature of their heme binding. Despite possessing the same heme prosthetic group, both enzymes differ in their heme affinity (*12*). The higher heme affinity of SBP than of HRP-C (*12*) is consistent with our observation of the higher thermal stability of the heme cavity in SBP. Hence, a stronger heme−apoprotein interaction in SBP than in HRP-C contributes to lowering the free energy of the native state of SBP to a greater extent, giving rise to a higher $\Delta G°(H_2O)$ value and an increased thermoresistance.

In heme proteins, the interaction of heme with several surrounding amino acids affects the folded tertiary structure near the heme site. Comparison of the structural features of the heme active sites of SBP and HRP-C shows two differences in the heme−apoprotein interactions (*7*). While one of the heme propionates is hydrogen bonded to glutamine (Gln176) in HRP-C, it is an arginine residue (Arg175) in SBP (*7*). Further, a direct van der Waals interaction between the C8 heme vinyl substituent and Met37 exists in SBP (Figure 1), which is so far not observed in other plant peroxidases (*7*), which Henriksen et al. (*7*) predicted could be the cause of the increased thermal stability and susceptibility to heme loss. Our experimental results rule out any significant contribution of hydrogen bonding in the extra stability of the heme pocket of SBP compared to that of HRP-C. Therefore, the extra stability of the heme pocket of SBP could predominantly be arising due to the Met37−heme interaction.

In our previous study (*18*), we reported that the fluorescence emission characteristics of Trp117 of apo-SBP and apo-HRP-C are very similar. In the study presented here, we report that their thermal and conformational stabilities are also comparable. These observations may be attributed to having no net difference in their inter-residue interactions, consistent with their high degree of sequence homology. We further reported (*18*) that SBP and HRP-C exhibit a difference in the magnitude of the picosecond tryptophan lifetime mainly due to the difference in their orientation factor, κ^2. This may be attributed to the combined effect of differences in their heme−apoprotein interactions, as observed in this study, and the tryptophan environmental polarity (*18*).

REFERENCES

1. Dunford, H. B., and Stillman, J. S. (1976) *Coord. Chem. Rev. 19*, 187−251.
2. Dunford, H. B. (1991) in *Peroxidases in Chemistry and Biology* (Everse, J., Everse, K. E., and Grisham, M. B., Eds.) Vol. II, pp 1−24, CRC Press, Boca Raton, FL.
3. Gillikin, J. W., and Graham, J. S. (1991) *Plant Physiol. 96*, 214−220.
4. Nissum, M., Feis, A., and Smulevich, G. (1998) *Biospectroscopy 4*, 355−364.
5. Gijzen, M. (1997) *Plant J. 12*, 991−998.
6. McEldoon, J. P., Pokora, A. R., and Dordick, J. S. (1995) *Enzymol. Microb. Technol. 17*, 359−365.
7. Henriksen, A., Mirza, O., Indiani, C., Teilum, K., Smulevich, G., Welinder, K. G., and Gajhede, M. (2001) *Protein Sci. 10*, 108−115.
8. Gajhede, M., Schuller, D. J., Henriksen, A., Smith, A. T., and Poulos, T. L. (1997) *Nat. Struct. Biol. 4*, 1032−1038.
9. Nissum, M., Schiødt, C. B., and Welinder, K. G. (2001) *Biochim. Biophys. Acta 1545*, 339−348.
10. Tsaprailis, G., Chan, D. W. S., and English, A. M. (1998) *Biochemistry 37*, 2004−2016.
11. Chattopadhyay, K., and Mazumadar, S. (2000) *Biochemistry 39*, 263−270.
12. McEldoon, J. P., and Dordick, J. S. (1996) *Biotechnol. Prog. 12*, 555−558.
13. Bassi, A. S., Rao, K. J., Kandula, S., and Gijzen, M. (2000) *J. Biochem. 127*, 239−245.
14. Kenausis, G., Chen, Q., and Heller, A. (1997) *Anal. Chem. 69*, 1054−1056.
15. Wang, B., Li, B., Wang, Z., Xu, G., Wang, Q., and Dong, S. (1999) *Anal. Chem. 71*, 1935−1938.
16. Wright, H., and Nicell, J. A. (1999) *Bioresour. Technol. 70*, 69−79.
17. Bedard, P., and Mabrouk, P. A. (1997) *Biochem. Biophys. Res. Commun. 240*, 65−67.
18. Kamal, J. K. A., and Behere, D. V. (2001) *Biochem. Biophys. Res. Commun. 289*, 427−433.
19. Elving, P. J., Markowitz, J. M., and Rosenthal, I. (1956) *Anal. Chem. 28*, 1179−1180.

20. Furhop, J. H., and Smith, K. M. (1975) Laboratory methods, in *Porphyrins and Metallo porphyrins* (Smith, K. M., Ed.) pp 757−869, Elsevier, Amsterdam.
21. Teale, F. W. J. (1959) *Biochim. Biophys. Acta 35*, 543.
22. Mach, H., Middaugh, C. R., and Lewis, R. V. (1992) *Anal. Biochem. 200*, 74−80.
23. Lakowicz, J. R. (1999) in *Principles of Fluorescence Spectroscopy*, 2nd ed., Kluwer/Plenum, New York.
24. Jocelyn, P. C. (1987) *Methods Enzymol. 143*, 246−256.
25. Pace, C. N. (1986) *Methods Enzymol. 131*, 266−280.
26. Agashe, V. R., and Udgaonkar, J. (1995) *Biochemistry 34*, 3286−3299.
27. Ionescu, R. M., Smith, V. F., O'Neill, J. C., Jr., and Matthews, C. R. (2000) *Biochemistry 39*, 9540−9550.
28. Lumry, R., and Eyring, H. (1954) *J. Phys. Chem. 58*, 110−120.
29. Freire, E. (1995) *Methods Enzymol. 259*, 144−168.
30. Pappa, H. S., and Cass, A. E. G. (1993) *Eur. J. Biochem. 212*, 227−235.
31. Hawkes, R., Grutter, M. G., and Schellman, J. (1984) *J. Mol. Biol. 175*, 195−212.
32. Schmitz, N., Gijzen, M., and van Huystee, R. (1997) *Can. J. Bot. 75*, 1336−1341.
33. Sessa, D. J., and Anderson, R. L. (1981) *J. Agric. Food Chem. 29*, 960−965.
34. Pace, C. N. (1990) *Trends Biochem. Sci. 15*, 14−17.
35. Vallée, B., Teyssier, C., Maget-Dana, R., Ramstein, J., Bureaud, N., and Schoentgen, F. (1999) *Eur. J. Biochem. 266*, 40−52.
36. Honig, B., and Yang, A.-S. (1995) *Adv. Protein Chem. 46*, 27−58.
37. Creighton, T. E. (1993) in *Protein Structures and Molecular Principles*, 2nd ed., Freeman, New York.
38. Fitter, J., Herrmann, R., Dencher, N. A., Blume, A., and Hauss, T. (2001) *Biochemistry 40*, 10723−10731.
39. Frausto da Silva, J. J. R., and Williams, R. J. P. (1991) in *The Biological Chemistry of Elements, The inorganic chemistry of life*, pp 174, Clarendon Press, Oxford, U.K.

BI025621E